Recent Work in the MFEM Miniapps for Shock Hydro, Field Remap, and Mesh Optimization

MFEM Community Workshop

October 23, 2024

CASC
Center for Applied Scientific Computing

V. Tomov on behalf of the MFEM team

LLNL-PRES-870871
This work was performed under the auspices of the U.S. Department of Energy by Lawrence Livermore National Laboratory under contract DE-AC52-07NA27344. Lawrence Livermore National Security, LLC

Lawrence Livermore National Laboratory

Laghos - LAGrangian High-Order Solver

Finite element solver for single-material Lagrangian hydrodynamics

```
       __                __
      / /   ____  ____  / /_  ____  _____
     / /   / __ `/ __ `/ __ \/ __ \/ ___/
    / /___/ /_/ / /_/ / / / / /_/ (__  )
   /_____/\__,_/\__, /_/ /_/\____/____/
               /____/
```

$$\frac{d\rho}{dt} = -\rho \nabla \cdot v, \qquad \frac{dx}{dt} = v$$

$$\rho \frac{dv}{dt} = \nabla \cdot \sigma, \qquad \rho \frac{de}{dt} = \sigma : \nabla v$$

- Resembles the main computational kernels without the additional physics code.
- Separation between FE assembly and physics-related computations.
- Captures the basic structure of many other compressible shock hydrocodes.
- Publicly available C++ code with domain-decomposed MPI parallelism.

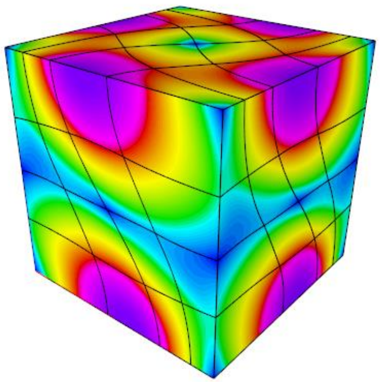

3D Taylor-Green smooth test problem

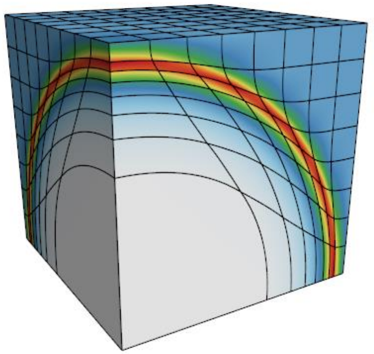

3D Sedov explosion shock test problem

High-Order Curvilinear Finite Element Methods for Lagrangian Hydrodynamics, Dobrev, Kolev, Rieben, 2012.

Goal: enable hydro simulations in curved domains

- Sedov simulation:
  $E_0 = 0.25, t = 0.6$

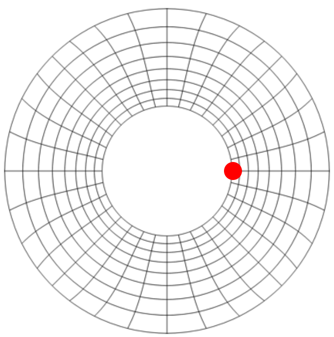

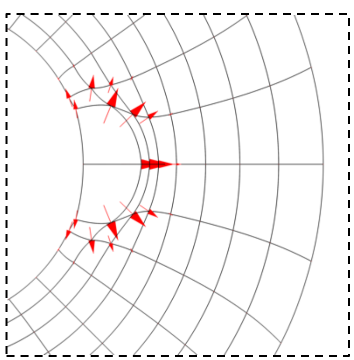

$\boldsymbol{v} = \boldsymbol{0}$

$\boldsymbol{v} \cdot \boldsymbol{n} = 0$

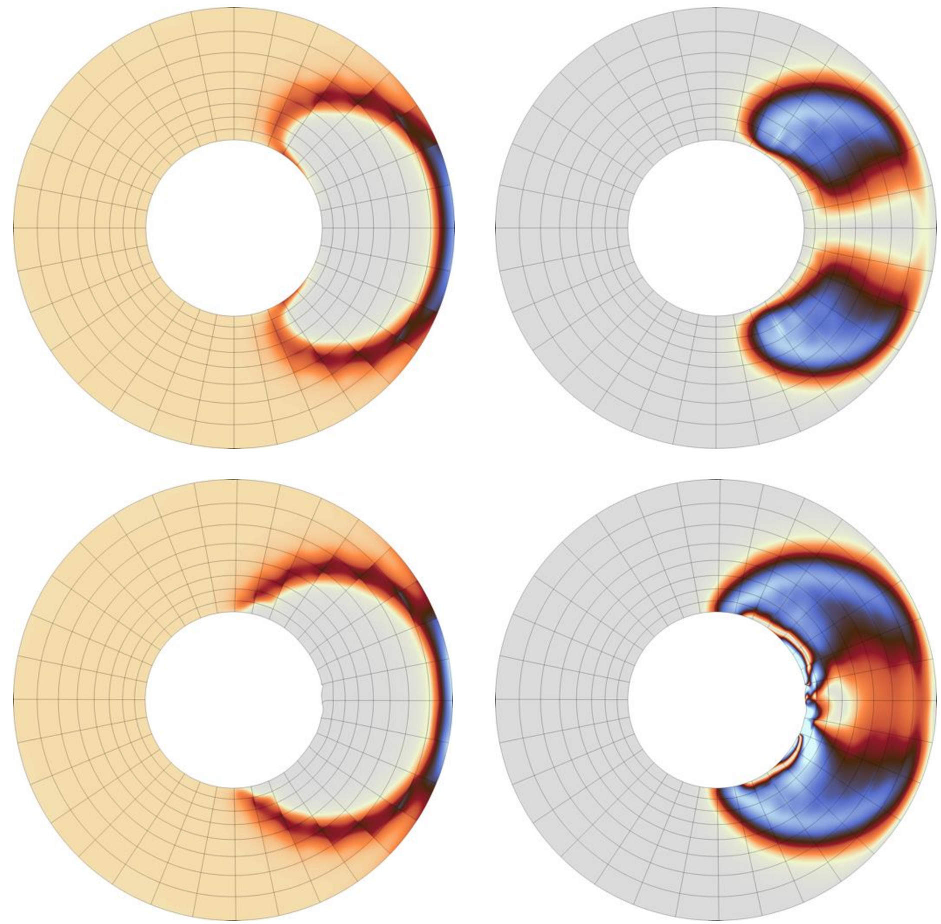

Final density

Final velocity

Weak enforcement of free-slip wall BC $(\boldsymbol{v} \cdot \boldsymbol{n} = 0)$

- The explicit evolution requires penalizing both the normal velocity $\boldsymbol{v} \cdot \boldsymbol{n}$ and normal acceleration $\dot{\boldsymbol{v}} \cdot \boldsymbol{n}$. Derived by Nabil Atallah.

$$(\rho\, \dot{\boldsymbol{v}}, \boldsymbol{w}_i)_{\Omega(t)} + (\alpha_0\, \rho_{\max}\, L\, \dot{\boldsymbol{v}} \cdot \boldsymbol{n}_0\,,\, \boldsymbol{w}_i \cdot \boldsymbol{n}_0)_{\Gamma_0} +$$
$$(\boldsymbol{\sigma}, \nabla \boldsymbol{w}_{i;})_{\Omega(t)} + (\beta\, \rho\, c_s\, \boldsymbol{v} \cdot \boldsymbol{n}\,,\, \boldsymbol{w}_i \cdot \boldsymbol{n})_{\Gamma(t)} = 0$$

$\alpha_0 = \beta\, L / J^{1/d}_{\hat{x} \to x_0}$

Maintains magnitude under ref

Trace inequality based constant

Unit consistency

Time independence (won't matter with PA)

- The internal energy term follows directly:

$$(\rho\, \dot{e}, \phi_l)_{\Omega(t)} - (\boldsymbol{\sigma} : \nabla \boldsymbol{v}, \phi_l)_{\Omega(t)} - (\beta\, \rho\, c_s\, (\boldsymbol{v} \cdot \boldsymbol{n})^2, \phi_l)_{\Gamma(t)} = 0$$

- Mass matrices are still constant in time.
- Mass / momentum / total energy are conserved as in the original method.

Weak Boundary Conditions for Lagrangian Shock Hydrodynamics: A High-Order Finite Element Implementation on Curved Boundaries, Atallah, Tomov, Scovazzi, 2023.

The new BC terms don’t affect the standard tests

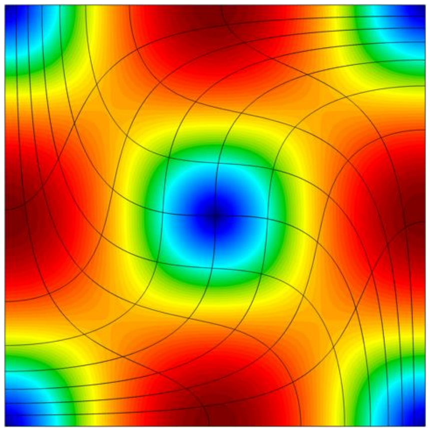

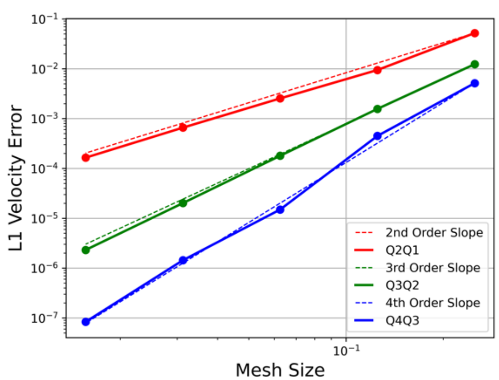

Expected convergence for smooth Taylor-Green

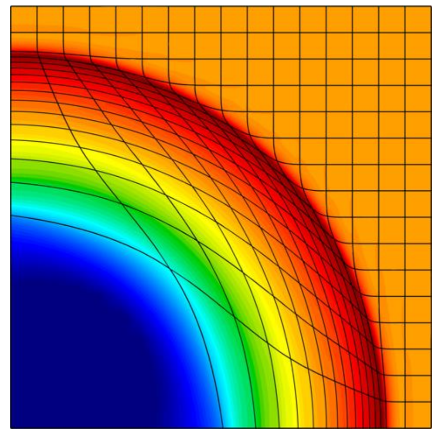

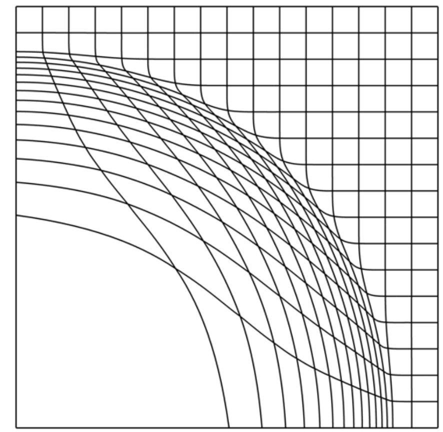

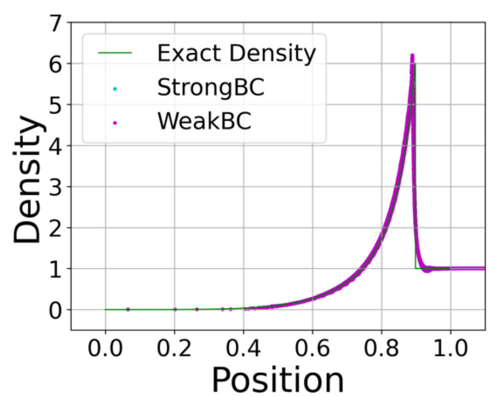

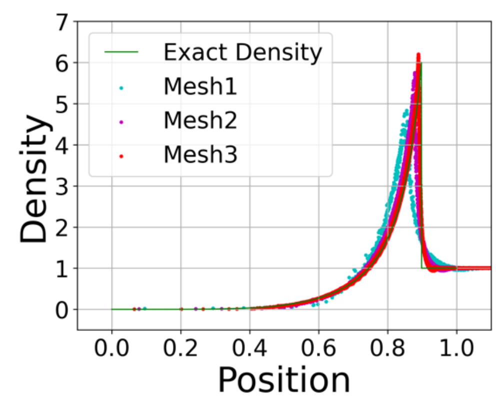

Expected shock positions for the Sedov tests

The method was tested in various 2D/3D setups

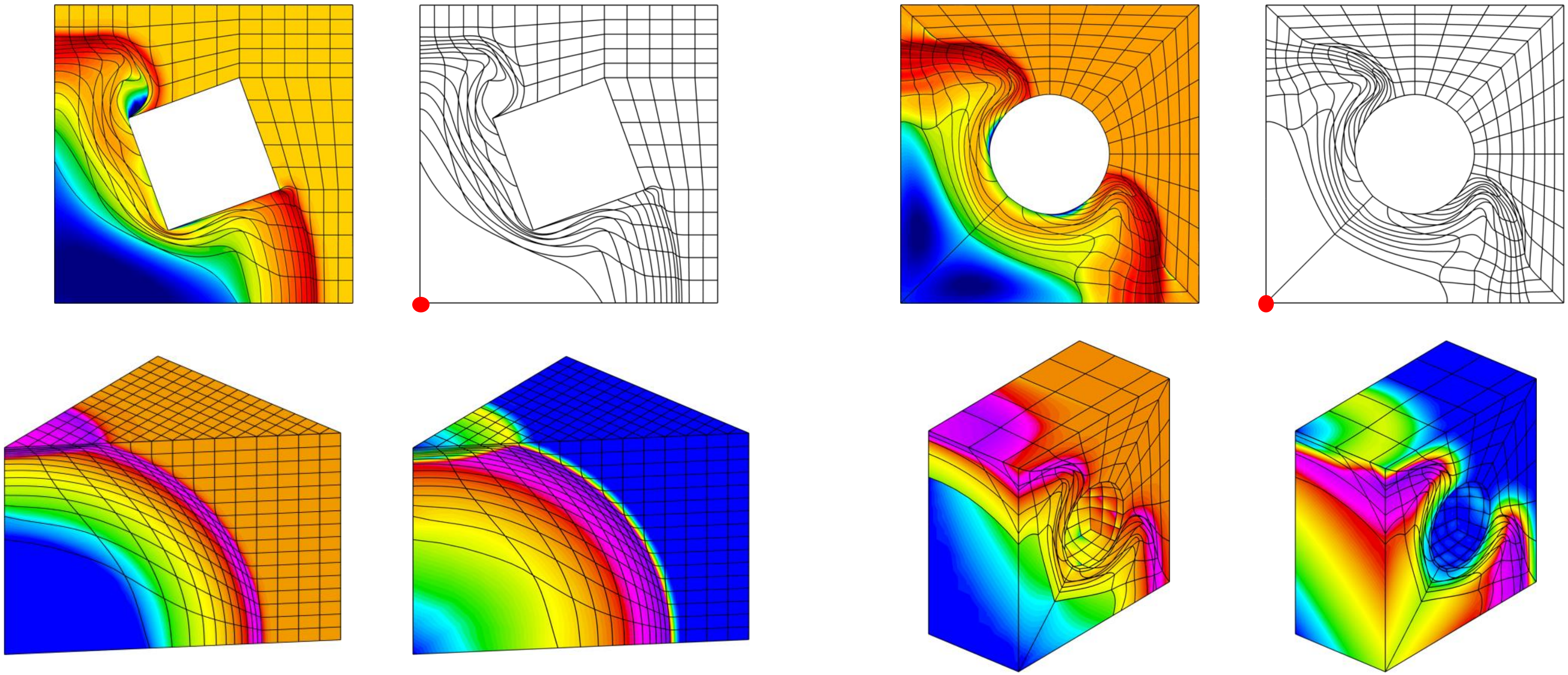

Weak Boundary Conditions for Lagrangian Shock Hydrodynamics: A High-Order Finite Element Implementation on Curved Boundaries, Atallah, Tomov, Scovazzi, 2023.

New release of Laghos is coming up!

Ongoing research: shifted wall boundary conditions on embedded grids

- The BC is enforced in a conforming face through a Taylor expansion.

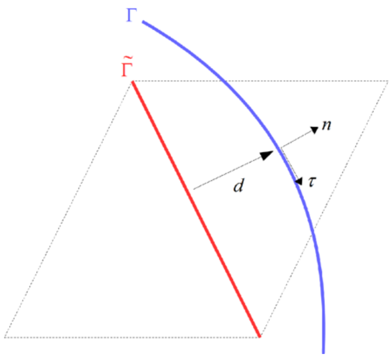

$$v.n = 0$$

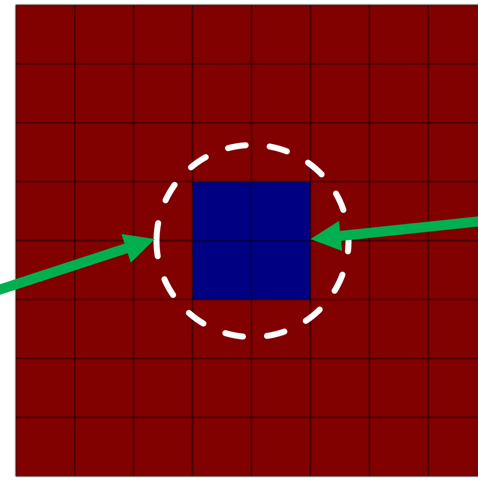

$$(v + \sum_{i=1}^{m} \frac{D_d v}{i!}).n = 0$$

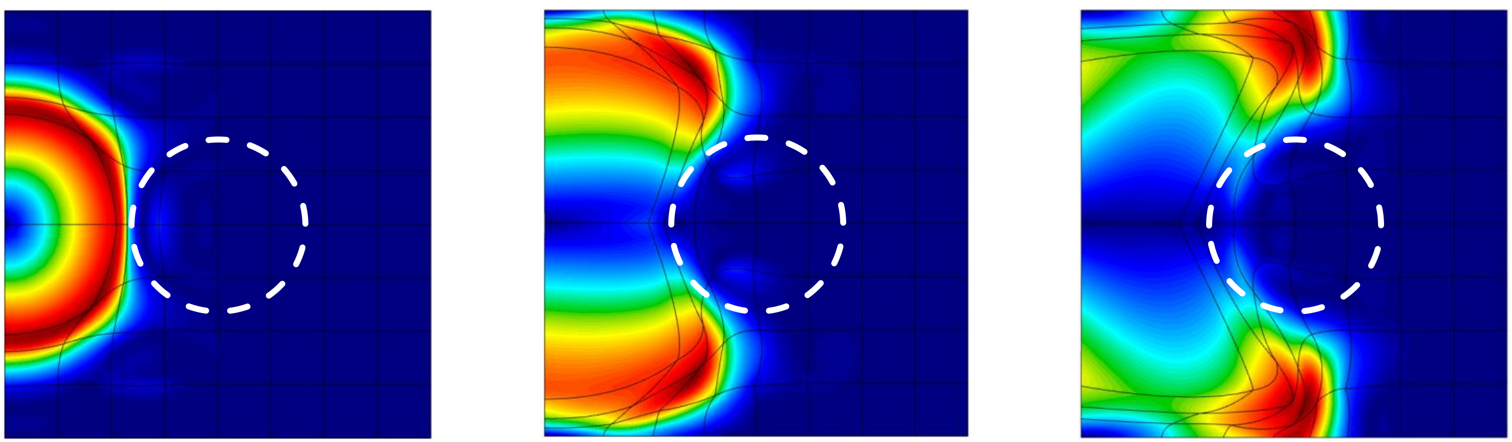

Sedov on an embedded circular obstacle, t = 0, t = 0.45, t = 0.8.

Shifted Interface Method for 2-material Lagrangian hydrodynamics

- Interface conditions are posed on the continuous PDE level:

$$[\![p]\!] = p^+ \boldsymbol{n}^+ + p^- \boldsymbol{n}^- = 0 \qquad [\![\boldsymbol{v}]\!] = \boldsymbol{v}^+ \cdot \boldsymbol{n}^+ + \boldsymbol{v}^- \cdot \boldsymbol{n}^- = 0$$

- Proposed weak formulation:

$$\int_\Omega (\alpha_1\rho_1 + \alpha_2\rho_2)\frac{d\boldsymbol{v}}{dt} \cdot \boldsymbol{\psi} = \int_\Omega p\nabla \cdot \boldsymbol{\psi} + (1-\alpha_1)\int_{\Gamma_1} [\![\nabla p \cdot \boldsymbol{d}_1]\!] \cdot \boldsymbol{\psi} + (1-\alpha_2)\int_{\Gamma_2} [\![\nabla p \cdot \boldsymbol{d}_2]\!] \cdot \boldsymbol{\psi} - \int_\Omega \mu \nabla \boldsymbol{v}^s : \nabla \boldsymbol{\psi}$$

$$\int_\Omega \alpha_1\rho_1 \frac{de_1}{dt}, \phi = -\int_\Omega p\nabla \cdot \boldsymbol{v}, \phi + (1-\alpha_2)\int_{\Gamma_2} [\![((\nabla \boldsymbol{v}\boldsymbol{d}_2) \cdot \boldsymbol{n})\boldsymbol{n}]\!]\{p\phi\} + \int_\Omega \mu\nabla\boldsymbol{v}^s : \nabla\boldsymbol{v}\phi$$

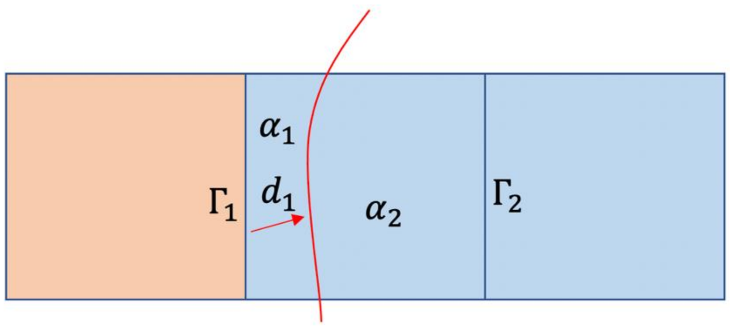

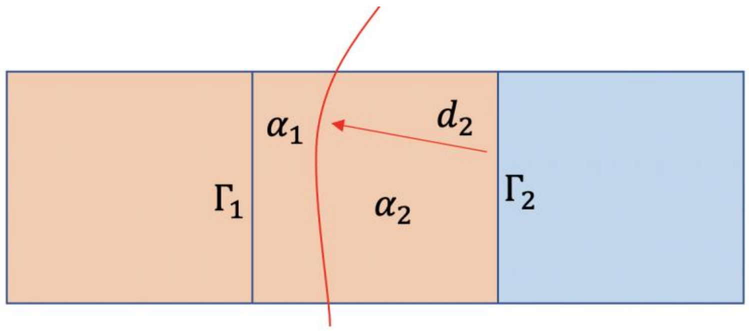

A High-Order Shifted Interface Method for Lagrangian Hydrodynamics, Atallah, Mittal, Scovazzi, Tomov, 2024.

Shifted Interface Method has been applied to 2-material Lagrangian hydrodynamics

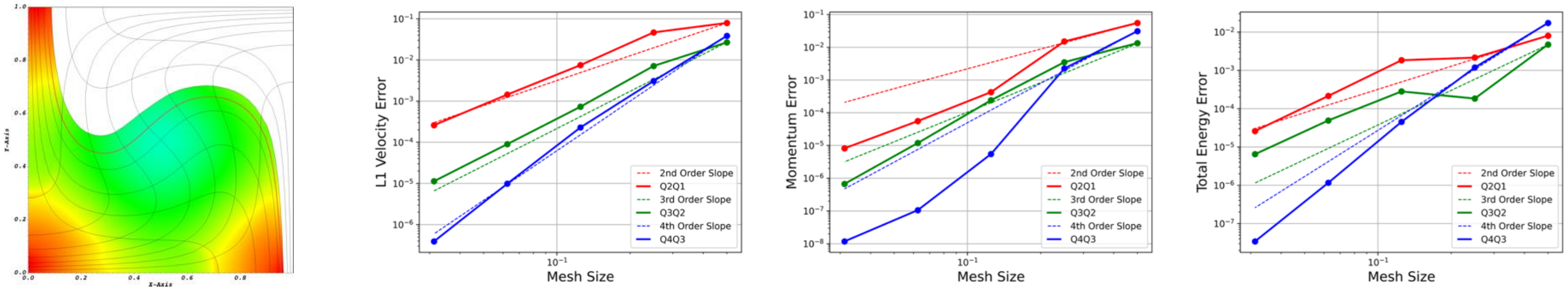

Convergence on a smooth test with an artificial interface

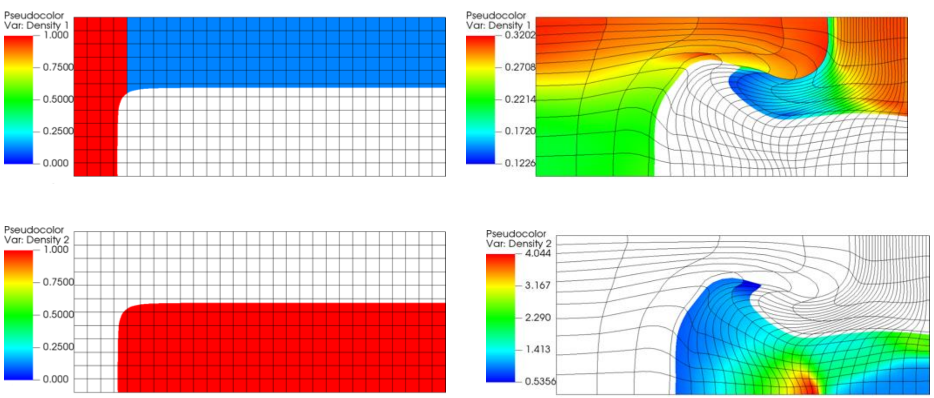

2D triple point problem with 2 materials

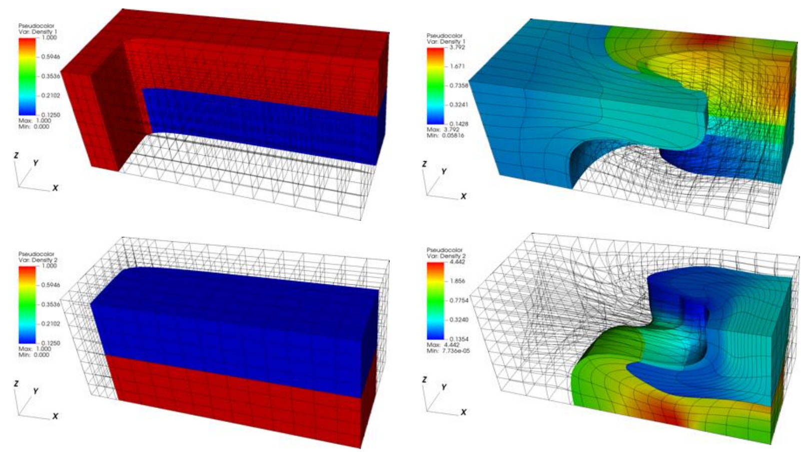

3D triple point problem with 2 materials

A High-Order Shifted Interface Method for Lagrangian Hydrodynamics, Atallah, Mittal, Scovazzi, Tomov, 2024.

Ongoing research: exact cut-cell integration for multi-material Lagrangian hydrodynamics

- Integration of implicit shapes.
  Specified by discrete level set functions.
  See example 38.
- Moments-based integration:
  Standard quad positions / compute weights.
  Reduces always to 1D integral computations.
  Native MFEM implementation by Jan-Phillip Bäcker.
- Algoim-based integration:
  Positions are based on the implicit domain.
  Ported to MFEM by B. Lazarov, K. Mittal.

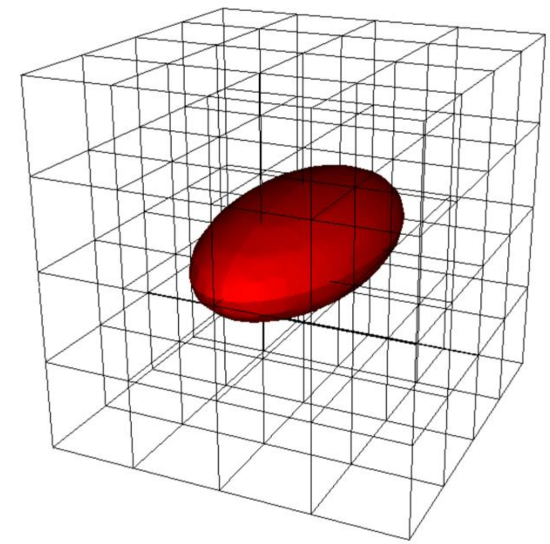

Integrated shape in Example 38

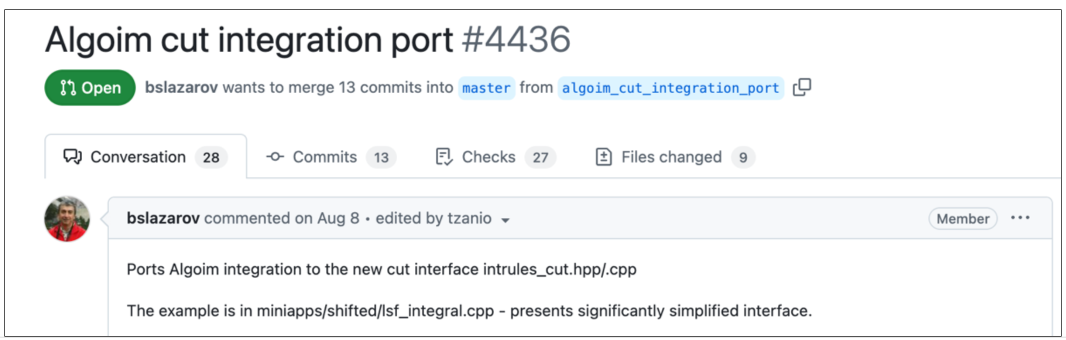

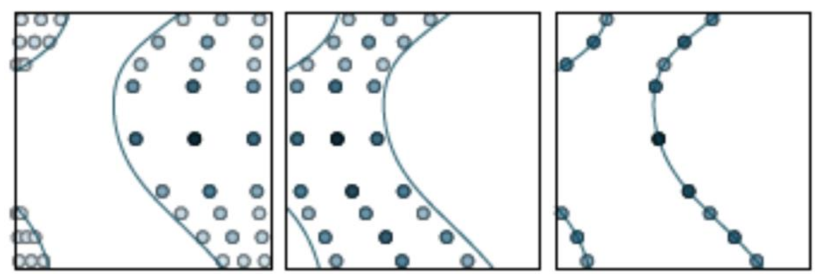

Algoim quadrature point locations

Remhos - REMap High-Order Solver

Finite element solver for advection-based remap of scalar fields

$$u = x_{final} - x_0$$

$$x(\tau) = x_0 + \tau u, \qquad \tau \in [0,1]$$

$$\frac{d\eta}{d\tau} = u \cdot \nabla \eta, \qquad \eta_0 = \eta(x_0)$$

Standard formulation of the pseudotime advection remap

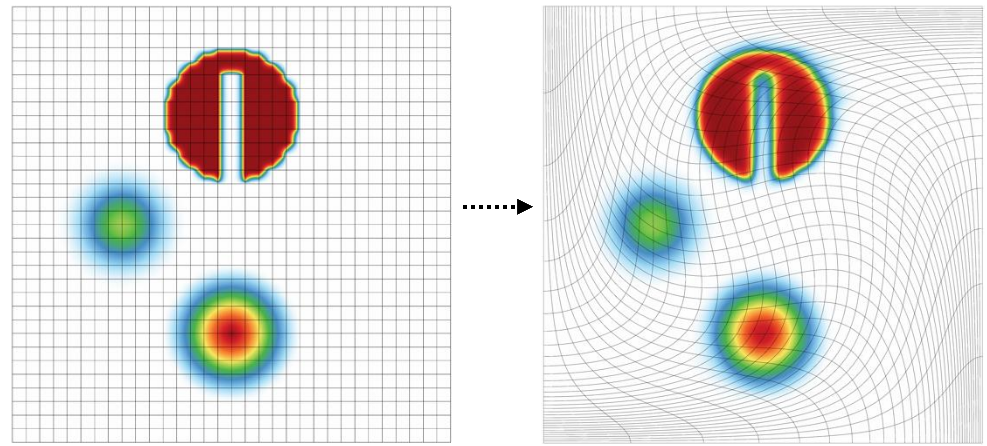

Remap benchmark result

- Requirements:
  - Conservation of mass.
  - Local bounds preservation.
  - High-order accuracy for smooth fields.

$$\frac{d}{d\tau}\int \eta = 0$$

$$\min_{j \in N_i} \eta_j^k \le \eta_i^{k+1} \le \max_{j \in N_i} \eta_j^k$$

- Finite element operations only; no computations of intersections, meshing, etc.

Monotonicity in high-order curvilinear finite element ALE remap, Anderson, Dobrev, Kolev, Rieben, 2015.

Issue: diffusion of small values (less than 1e-4) is characteristic of finite element methods

- The following gives good results … if one doesn't look at the log scale:
  - Discretization through arbitrary order FE, conservative weak form.
  - Bounds are guaranteed by utilizing a 1st-order solution step.
  - Sharpness is retained through a nonlinear FCT blending step.

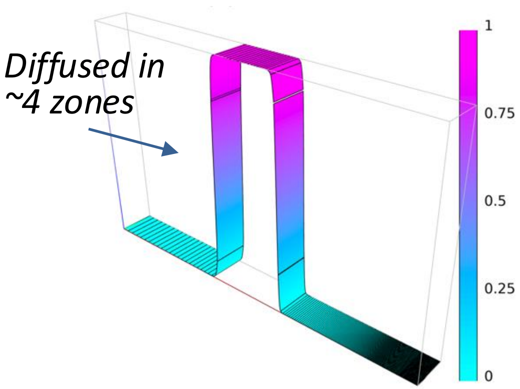

Preconditioned LO + state-of-art FCT blending (Kuzmin, Hajduk et al)

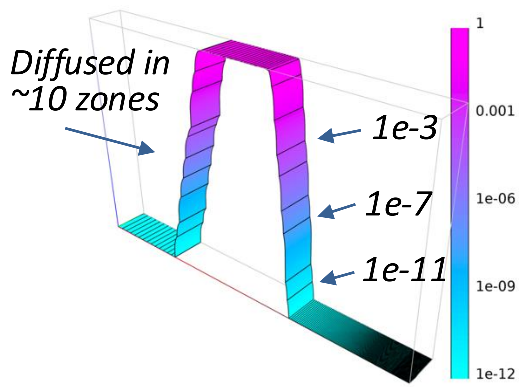

The same solution on logarithmic scale (our material cutoff is at 1e-12)

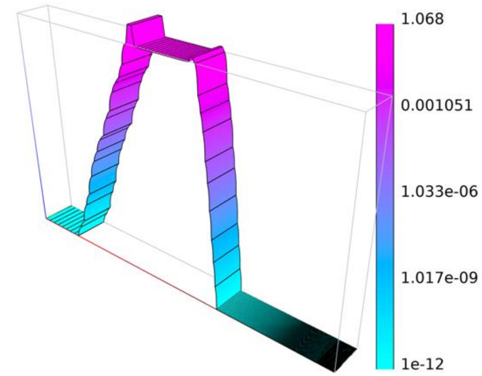

High-Order (unlimited) FE solution is what drives the propagation

- FCT does not help with this kind of diffusion, as it's present in the HO solution.

Propagation is reduced by decoupling the material velocity from the mesh motion

- Since the HO method is not good enough, we modify the PDE.
- Use the volume fraction specifics:
  - Values between 0 and 1 always represent numerical diffusion.
  - Transitions between 0 and 1 are monotone (no local extrema).
- Introduce a material propagation velocity u^*:
  u moves the mesh, u^* moves the material
  $u^* = u$ in pure material regions, when $\eta = 0$ or $\eta = 1$.
  $u^* \neq u$ in diffused regions, when $0 < \eta < 1$.

Continuous, normalized approximation of $\nabla\eta$

$$u^* = u - (1 - \eta^3)\ |u|\ d_{\nabla\eta}$$

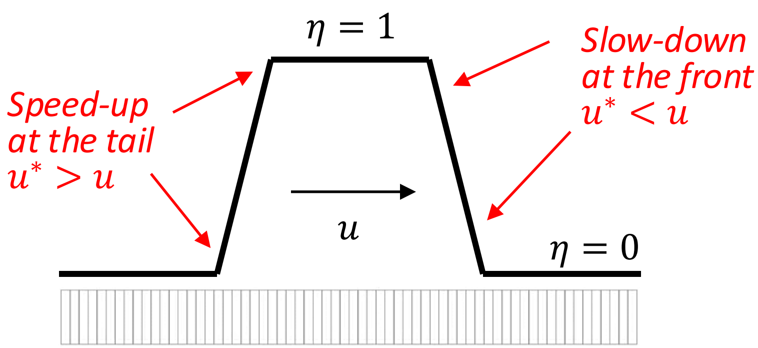

1D illustration - material frame

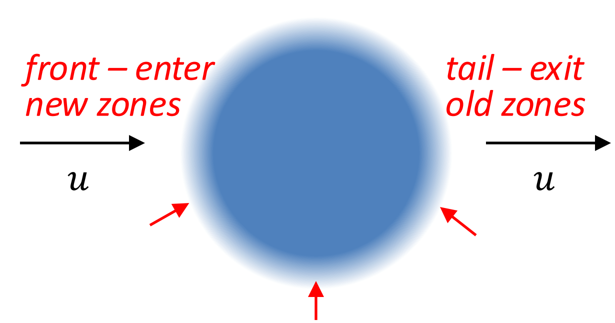

2D and 3D velocity modification – lab frame

Multi-material ALE remap with interface sharpening using high-order matrix-free FE methods, Vargas, Tomov, Rieben, 2024.

Propagation is reduced by decoupling the material velocity from the mesh motion

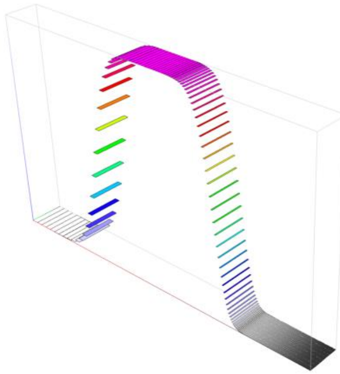

Unmodified velocity

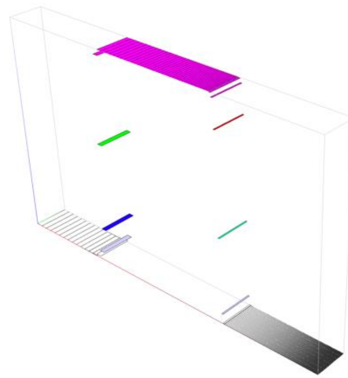

Modified velocity

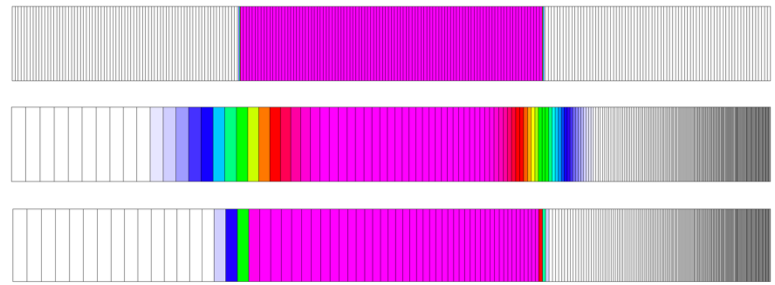

View from the top – IC / unmodified / modified

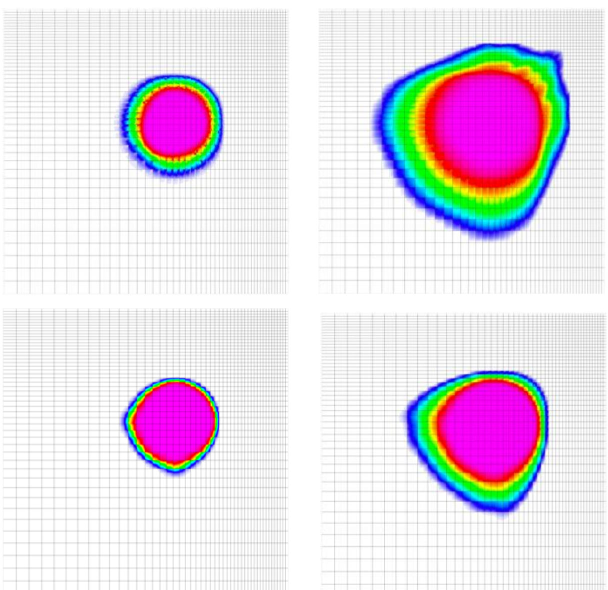

Original behavior:
Upwind + FCT

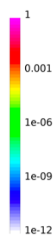

Modified:
Upwind + sharp

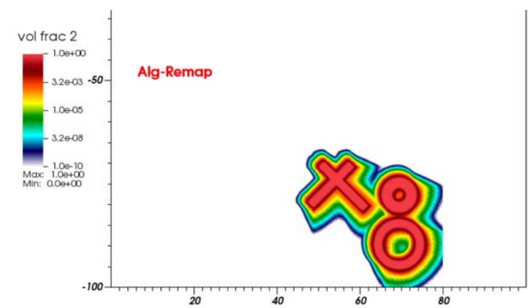

Original behavior:
Upwind + FCT

Modified:
Upwind + sharp

Advection remap for continuous FE fields

- Based on the Monolithic Convex Limiting (MCL) by Dmitri Kuzmin. Native MFEM implementation by Paul Moujaes. See example 9.

$$u_i^{new} = u_i^{old} + \frac{\Delta t}{m_i}\sum_j \left(d_{ij} - k_{ij}\right)\left(u_j^{old} - u_i^{old}\right) + a_{ij}\, f_{ij}$$

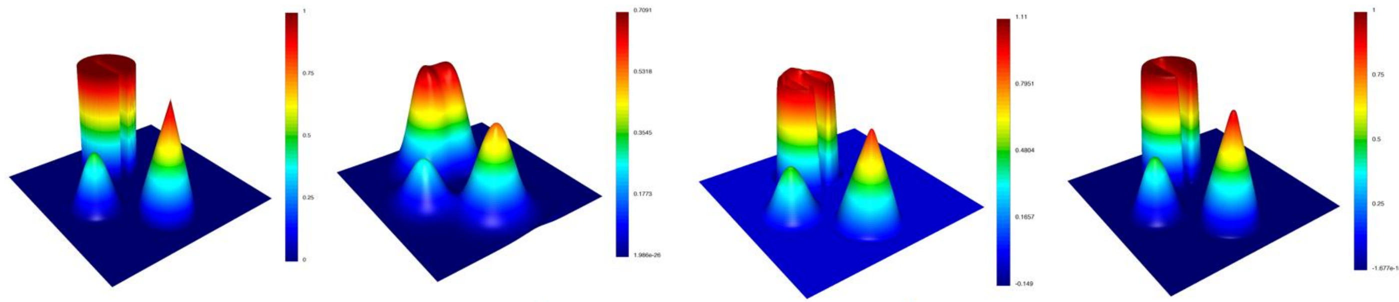

(a) Exact solution (b) Low-order ($a_{ij} = 0$) (c) High-order ($a_{ij} = 1$) (d) MCL (a_{ij} adaptive)

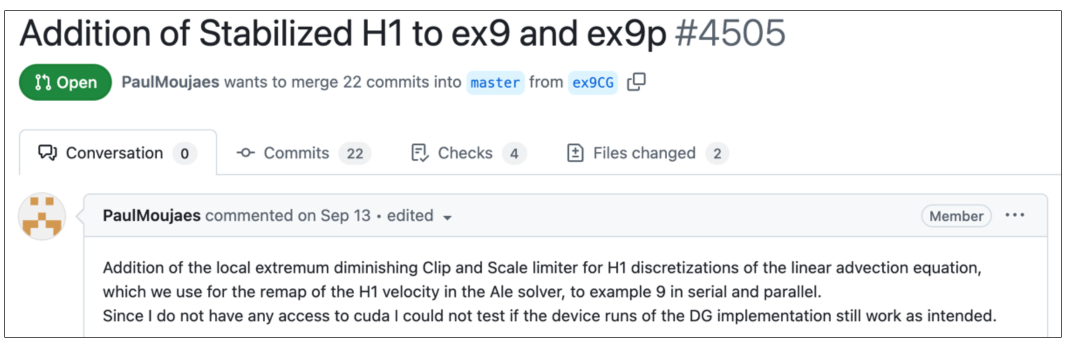

Addition of Stabilized H1 to ex9 and ex9p #4505

Open PaulMoujaes wants to merge 22 commits into master from ex9CG

Conversation 0 Commits 22 Checks 4 Files changed 2

PaulMoujaes commented on Sep 13 • edited Member

Addition of the local extremum diminishing Clip and Scale limiter for H1 discretizations of the linear advection equation, which we use for the remap of the H1 velocity in the Ale solver, to example 9 in serial and parallel.
Since I do not have any access to cuda I could not test if the device runs of the DG implementation still work as intended.

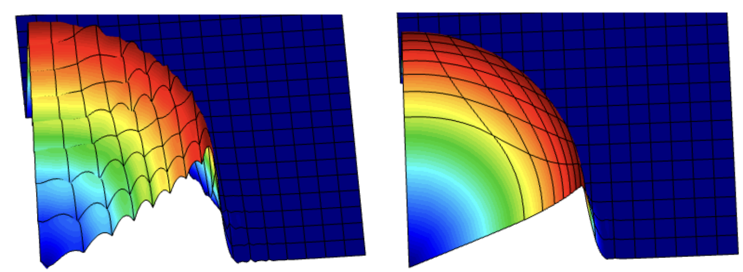

Velocity remap in Sedov ALE simulations

Monolithic convex limiting for continuous finite element discretizations of hyperbolic conservation laws, Kuzmin, 2020.

Ongoing research: optimization-based remap

- New LLNL project for performing remap for multi-material hydrodynamics.

c1. Produce accurate and sharp fields, i.e., introduce minimal numerical diffusion.
c2. Conserve momentum and material volume / mass / total energy.
c3. Preserve the local min and max bounds of all remapped fields.
c4. Maintain consistent material coupling, i.e., volume fractions must sum to one.

- Initial guess through GSLIB interpolation in physical space.

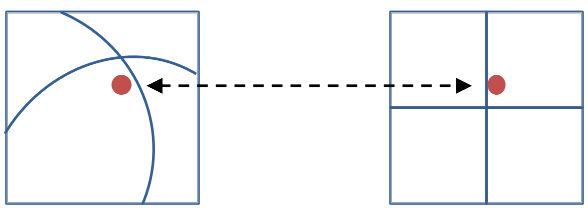

Deformed mesh   Optimized mesh

- Interior Point (IP) optimization.

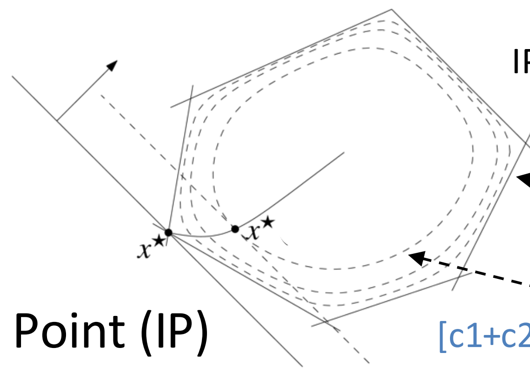

IP methods diagram

[c3] gives the region

[c1+c2] give the directions

- Latent Variable Proximal Point (LVPP) optimization. Solve in a latent space without bounds constraints.

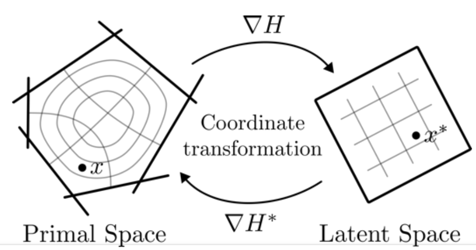

Mesh optimization miniapp

ethos

- Optimization by node movement.
  Target-Matrix Optimization Paradigm
  Variational minimization, preserves topology.

Based on local Jacobian

$$\sum_{E\in\mathcal{M}} \int_{E_t} \mu(T(x_t))$$

Mesh quality metric

- Solution-based r-adaptivity.

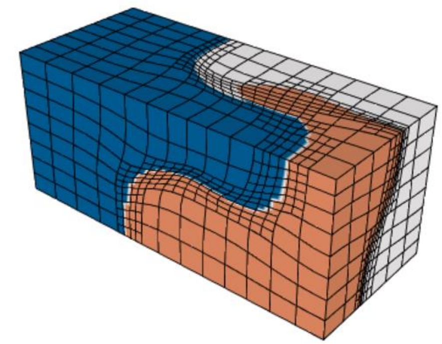

- Optimization by h-adaptivity.
  Still based on the TMOP targets.
  Applied to mesh opt by K. Mittal.

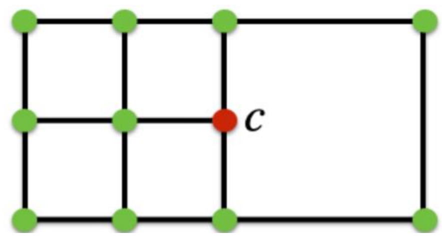

- Optimization by p-adaptivity.
  Applied to surface fitting.
  Applied to mesh opt by K. Mittal.

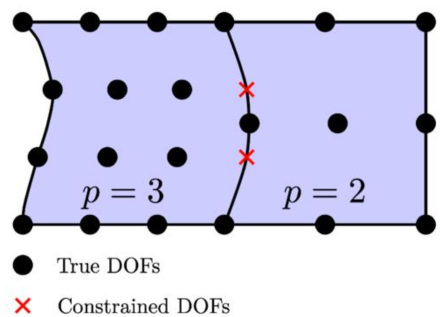

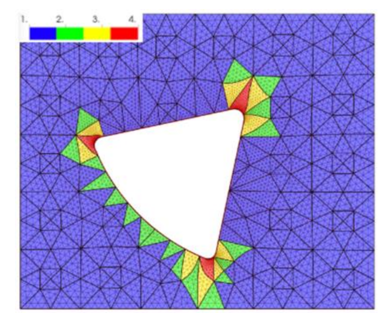

The Target-Matrix Optimization Paradigm for High-Order Meshes, Dobrev, Knupp, Kolev, Mittal, Tomov, 2019.
Mixed-Order Meshes Through rp-Adaptivity for Surface Alignment to Implicit Geometries, Mittal et al, 2024.

Surface fitting to implicitly defined interfaces

$$F(\mathbf{x}) = \sum_{E\in\mathcal{M}} \int_{E_t} \mu(T(x))dx_t + w_\sigma \sum_{s\in S} \sigma^2(x_s)$$

σ– Level set function *$\mathcal{S}$– Nodes for fitting* *w_σ – Fitting weight*

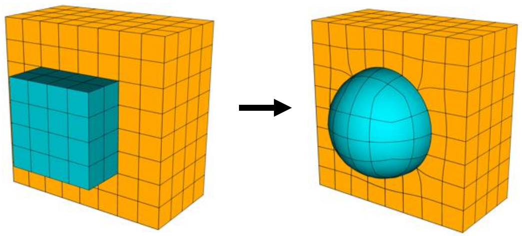

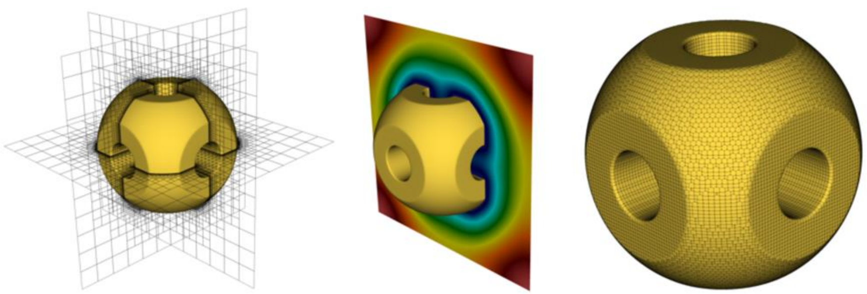

Fitting to a level set using a background mesh

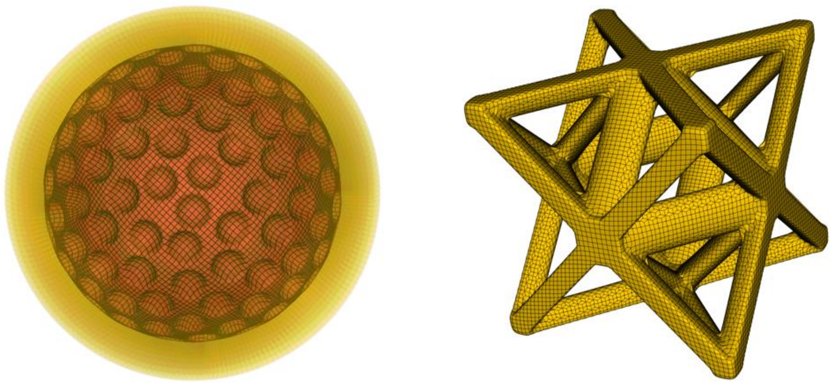

Fitting to a complex internal interface / boundary

- Mostly based in FE operations. Allows partial assembly and GPU execution.

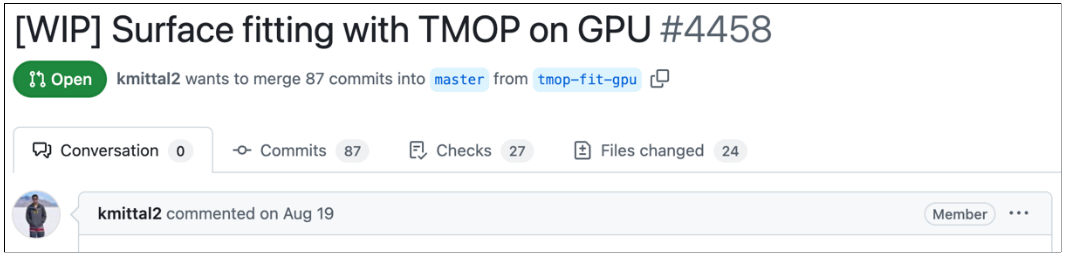

High-Order Mesh Morphing for Boundary and Interface Fitting to Implicit Geometries, Mittal et al, 2023.

Tangential relaxation for analytic surfaces

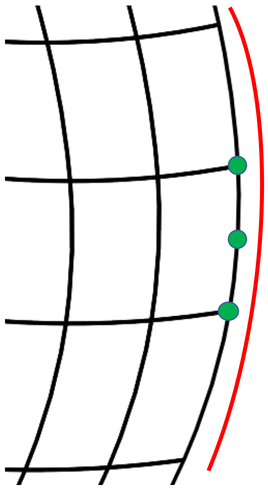

- The original DOFs are replaced by the parametrization DOFs.
  - The Newton solver operates on the new DOFs.

  2D curve DOFs: $Q(x, y) = t$

  3D surface DOFs: $Q(x, y, z) = (u, v)$

  3D edge DOFs: $Q(x, y, z) = t$

Q^{-1}

- Derivatives (2D curve): $$\frac{\partial F}{\partial t} = \ldots \frac{\partial \mu}{\partial T}\left(\frac{\partial T}{\partial x}\frac{\partial x}{\partial t} + \frac{\partial T}{\partial y}\frac{\partial y}{\partial t}\right)$$

- The original node positions may not be on the curve.

Inexact nodes move tangentially w.r.t. the analytic curve

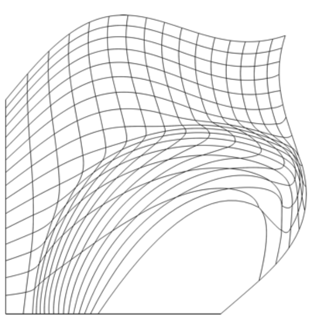

Initial mesh

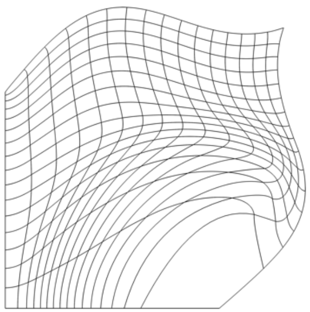

Optimized, d = 0.05

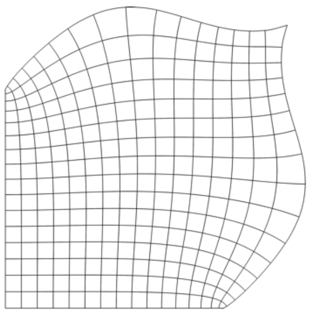

Fully optimized

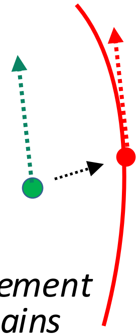

The displacement error remains

Ongoing research: PDE-driven mesh adaptivity with TMOP and AD

- Find mesh positions that gives an optimal PDE approximation.
  The mesh is optimized by node movement (r-refinement).

$$\min_{\mathrm{x}} \; \mathcal{F}_\mu(\mathrm{x}) + w\mathcal{F}_\mathrm{u}(\mathrm{x}, \mathrm{u}(\mathrm{x})) \qquad \mathcal{F}_\mathrm{u}(\mathrm{x}, \mathrm{u}(\mathrm{x})) = \int_\Omega (\mathrm{u} - \mathrm{u}^*)^2 \, d\Omega$$

- Gradient computation by reverse mode sensitivity. Work by Mathias Schmidt.

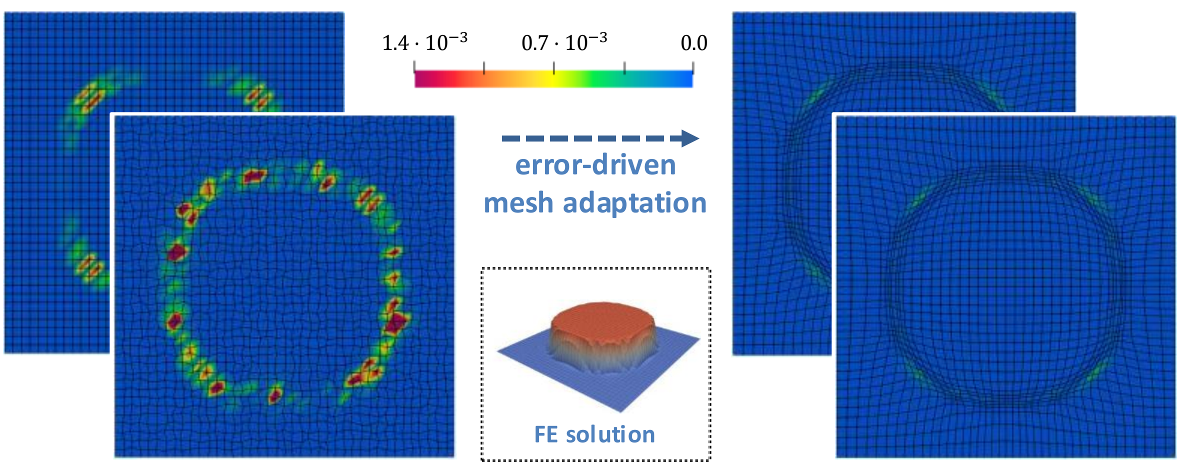

FE errors - initial meshes

FE errors - optimized meshes

Summary

- Laghos (shock hydro).
  - wall BC in curved domains.
  - shifted boundary and interface methods.
  - exact cut integration for immersed interfaces.

- Remhos (field remap).
  - sharpening of diffused interfaces.
  - stabilized H1 remap.
  - optimization-based multi-material remap.

- Mesh optimization.
  - r/h/p-adaptivity.
  - surface fitting to implicit geometries.
  - tangential relaxation for analytic surfaces.
  - PDE-driven mesh adaptivity.

CASC

Center for Applied Scientific Computing

Lawrence Livermore National Laboratory

Disclaimer

This document was prepared as an account of work sponsored by an agency of the United States government. Neither the United States government nor Lawrence Livermore National Security, LLC, nor any of their employees makes any warranty, expressed or implied, or assumes any legal liability or responsibility for the accuracy, completeness, or usefulness of any information, apparatus, product, or process disclosed, or represents that its use would not infringe privately owned rights. Reference herein to any specific commercial product, process, or service by trade name, trademark, manufacturer, or otherwise does not necessarily constitute or imply its endorsement, recommendation, or favoring by the United States government or Lawrence Livermore National Security, LLC. The views and opinions of authors expressed herein do not necessarily state or reflect those of the United States government or Lawrence Livermore National Security, LLC, and shall not be used for advertising or product endorsement purposes.